Sonar attenuation modeling for classification of marine sediments

Lester R. LeBlanc, Satchidanan Panda, and Steven G. Schock
Department of Ocean Engineering, Florida Atlantic University, Boca Raton, Florida 33431

(Received 5 April 1991; accepted for publication 30 August 1991)

An attenuation-based model for classification of marine sediments is developed for the chirp sonar operating in the frequency range of 2–10 kHz. A relaxation-time model is proposed that combines the various dissipative energy loss mechanisms of sound in marine sediments into a single parameter. Historical data were analyzed by converting attenuation values reported in "dB/m@kHz" to a single relaxation time value. Analysis of these previous attenuation measurements supports the use of a relaxation-time model. Based on this large collection of data, an empirical equation is developed that relates relaxation time to grain size (in phi units). Using this model, very little phase dispersion is observed for a correlated chirp pulse traveling through 40 m of sand, silt, or clay. Yet, this is not so for a pulse in the ultrasonic frequency range (0.2–1.0 MHz) traveling through only 10 cm of clay. Here, significant dispersion is noted. Because of the unique Gaussian-like shape of the correlated chirp pulse power spectrum, pulse elongation due to attenuation is minimized. Using the center frequency shift in the pulse spectrum, a new "instantaneous frequency" method of attenuation estimation is proposed that overcomes the problems associated with interfering reflections. Based on the relaxation-time model, the correlated chirp pulse was synthetically attenuated to establish a relation between the relaxation time and the center frequency shift. *In situ* sediment-type predictions from chirp sonar data using the instantaneous frequency method and analyses of core samples taken in the Narragansett Bay, Rhode Island are in good agreement.

PACS numbers: 43.30.Ma, 43.30.Tg

INTRODUCTION

Over the past two decades of marine sub-bottom exploration, the reflection profiling technique has been used primarily to delineate geological and stratification structures. Little has been done to use sub-bottom profilers to remotely classify sediments from attenuation estimates of the seafloor sediments. Sediment-type predictions from the surface reflection strength and impedance estimates have been attempted previously.[1–3] An accurate estimate of attenuation will provide supplementary and further insight to the geotechnical properties of the seafloor sediments. Also, knowledge of the variation of attenuation with frequency is essential to the study of dispersion and attenuation of sound in marine sediments. Experimental data on marine sediments differ in reporting both the values of attenuation coefficients, and the frequency dependence of attenuation. Also, similar controversies exist in the theoretical modeling of attenuation of sound in marine sediments. Detailed theoretical treatments of sound propagation in saturated sediments have been done by Biot,[4–7] Stoll and Bryan,[8] and Stoll.[9] But these analyses are complex and do not provide an easy experimental means of evaluating the parameters characterizing the attenuation behavior in marine sediments. We are in pursuit of a simple and reliable method of modeling attenuation in marine sediments. The model developed herein is robust and verified by experimental data. Also, the model provides us with insight to develop a suitable attenuation estimation technique for rapid determination of sediment attenuation on the site.

Several attenuation measurement techniques have been proposed both in the time and frequency domains, namely, rise-time,[10–12] spectral ratio,[10–14] spectral shift,[15,16] and wavelet-modeling techniques.[12,17] For the upper few meters of the seafloor, which is usually layered, these methods fail to provide a satisfactory attenuation estimate. For the spectral ratio method, errors are caused by overlapping reflections that produce notches in the spectral estimates of the time-gated samples taken from the record. Similar problems exist for the time domain methods. Due to the lack of a robust attenuation estimation technique, and discrepancies in the published attenuation data, it is difficult to identify marine sediments by *in situ* measurement of attenuation coefficient.

We have developed an attenuation model based on a relaxation mechanism for use in a sediment classification scheme that can be implemented in real time. The relaxation-time model shows good agreement with existing experimental data. A relation between relaxation time and sediment type is established, and is used to predict seafloor sediments. Also, a new time domain technique to experimentally estimate the attenuation of sound in sediments is developed. Sediment-type predictions using attenuation estimates from chirp sonar data taken in Narragansett Bay, RI, are in good agreement with nearby cores.

I. ATTENUATION MODEL

It is well known that fully saturated marine sediments exhibit a relaxation phenomenon. The relaxation time is a measure of the finite time needed to change the density by application of a sudden pressure. Different attenuation processes such as viscous loss, solid friction, and thermoelastic relaxation have been suggested. Each of these processes might exhibit its own relaxation time. Here, we take a simplified view of the attenuation mechanism. We assume, for the limited frequency range used in sub-bottom profiling, a marine sediment is macroscopically homogeneous and many different relaxation times can be lumped into a single relaxation time. With the knowledge of the relaxation time, the response of the attenuating medium can be completely characterized. The mathematical details for a relaxation-time model can be found in the literature.[18] However, a brief description is included here for convenience.

The equation of state for a relaxation-time model is given by

$$p = V^2\rho + R\dot{\rho}, \tag{1}$$

where p is the excess pressure, ρ is the excess density, V is the adiabatic sound speed, and R is a constant characterizing the relaxation process. Combining the equation of state with the equation of continuity and the momentum equation, the equation of motion becomes

$$\ddot{\xi} = V^2\left(\frac{\partial^2\xi}{\partial x^2} + \tau\rho\frac{\partial\dot{\xi}}{\partial x}\right), \tag{2}$$

where $\tau = R/V^2$ is the relaxation time and x is the direction of motion. The well-known solution to Eq. (2) is a damped plane harmonic wave given by

$$\xi = \xi_0 e^{-\alpha x} e^{j(\omega t - kx)}, \tag{3}$$

where α is the attenuation coefficient and k is the wave number. Substitution of Eq. (3) into Eq. (2) yields

$$k^2 - \alpha^2 = \omega^2/V^2(1 + \omega^2\tau^2), \tag{4}$$

and

$$2\alpha k = \omega^3\tau/V^2(1 + \omega^2\tau^2). \tag{5}$$

By solving for the wave number and the attenuation coefficient, we obtain

$$\alpha = \omega^2\tau V_p/2V^2(1 + \omega^2\tau^2) \tag{6}$$

and

$$k = \omega/V_p, \tag{7}$$

where V_p, the phase velocity, is given by

$$V_p = (\sqrt{2}V/\omega\tau)\left[(1 + \omega^2\tau^2)(\sqrt{1 + \omega^2\tau^2} - 1)\right]^{1/2}. \tag{8}$$

For low frequency, that is, for $\omega\tau \ll 1$,

$$V_p \approx V(1 + 3\omega^2\tau^2/8 + \cdots). \tag{9}$$

Neglecting the second- and higher-order terms, we obtain

$$\alpha \approx \omega^2\tau/2V. \tag{10}$$

For low frequency, the attenuation coefficient varies as the square of the frequency. For sands, having a relaxation time of $\tau = 0.16\ \mu$s (as discussed later), a square-law frequency dependence can be used for the frequency range of 0–100 kHz without introducing more than 1% error. It is interesting that the attenuation value given by Eq. (10) is inversely proportional to the speed of sound. Thus, at low frequencies (< 100 kHz), relaxation time can be measured experimentally without requiring the knowledge of the speed of sound in the sediment sample. If one assumes a nominal speed of sound in the seafloor sediment, say 1500 m/s, depending on the sediment type, a small error will occur in calculating the distance traveled by using the measured time of flight method. By recasting Eq. (10), and using the result to calculate relaxation time, an equal and opposite error will occur. Equivalently, Eqs. (10) and (3) can be combined to express the loss of pulse amplitude solely as a function of frequency, time of flight, and relaxation time without any dependence on the distance x traveled by the pulse. The result is a simple relationship that allows us to calculate relaxation time using the measured time of flight and measured attenuation of peak amplitude of the correlated chirp pulse:

$$\tau = (2/t_x\omega^2)\ln|A_1/A_2|, \tag{11}$$

where t_x is the time of flight, and A_1, A_2 are the start and finish values of peak pulse amplitude. This equation assumes that phase dispersion is negligible, which will be shown later for the range of frequency of 2–10 kHz.

To model the attenuation of a broadband pulse, we use the frequency transfer function of the attenuating medium

$$H(\omega) = e^{-(\alpha + jk)x}. \tag{12}$$

The real part of the exponent represents attenuation of the pulse magnitude whereas the imaginary part represents time delay and phase dispersion of the pulse. If $S(\omega)$ is the Fourier transform of the input pulse $s(t)$, then the Fourier transform of the attenuated pulse $y(t)$ is obtained by

$$Y(\omega) = S(\omega)H(\omega). \tag{13}$$

The inverse Fourier transform of Eq. (13) provides us with the pulse time history after it has been modified by the attenuation and propagation delay occurring in the marine sediment:

$$y(t) = \int_{-\infty}^{\infty} S(\omega)H(\omega)e^{j\omega t}\,d\omega. \tag{14}$$

By using the relaxation-time method, the causal pulse $s(t)$ is propagated through the marine sediment in a manner predicted by the wave equation. This preserves the causal nature of the pulse. In practice, to predict the shape of a pulse after it has propagated causally through a marine sediment, Eq. (14) is evaluated numerically using a FFT method. An alternative method for predicting the phase dispersion of a pulse propagating causally would be to use the method described by Aki and Richards.[19] That is, for a causally propagating pulse, the phase spectrum can be obtained from the Hilbert transform of the log-amplitude spectrum of the attenuation filter. The resulting frequency-dependent wave number is then used to construct $H(\omega)$ without the requirement of satisfying the wave equation. This method, however, is difficult to implement numerically since it requires the evaluation of the Hilbert transform of a broadband process. The method is useful for modeling the effects of losses on pulse propagation when only the frequency dependent amplitude spectrum of attenuation is known. In our relaxation-time model, the phase velocity is derived directly from the wave equation and there is no further requirement to obtain a causal solution.

The above model for attenuation described in Eqs. (6) and (8) was used to relate some published experimental data on sediment attenuation to equivalent relaxation-time values. Later, Eq. (14) is used to develop a numerical procedure for measuring the effects of attenuation of sound in marine sediments on the correlated chirp sonar pulse operating in the frequency range of 2–10 kHz.

II. ANALYSIS OF EXPERIMENTAL DATA

Experimental data on compressional wave attenuation in marine sediments and corresponding geotechnical properties were collected to study the relaxation-time model. The data were published by Buchan *et al.*,[20] Hamilton *et al.*,[21–23] McCann and McCann,[24] and Shumway.[25] To verify the linear frequency dependence of attenuation, as suggested by some authors,[21–23] the attenuation coefficient in dB/m/kHz was evaluated from the collected data. The single most important geotechnical property that should correlate with attenuation is expected to be the mean grain diameter. In an attempt to establish this correlation, the attenuation in dB/m/kHz is plotted against the mean grain diameter in phi units (Fig. 1). The data is widely scattered and yet appears to show two separate groupings. Particularly, the data from Buchan *et al.*[20] and McCann and McCann,[24] measured at high frequency (>200 kHz), are offset from Hamilton's low-frequency data[21–23] (<50 kHz) by a large margin. We believe that the discrepancy is because the measurements were done at widely different frequencies and an assumption of linear frequency dependence is not correct. Next, the attenuation data in dB/m@kHz were converted to the relaxation time by solving for τ in Eq. (6). The relaxation time is plotted versus mean grain diameter for each sample (Fig. 2). As a result of converting the attenuation data to relaxation values, the scatter is significantly reduced. Especially, the data from Buchan *et al.*[20] and McCann and McCann,[24] obtained at 580–615 and 368 kHz, respectively, have fallen into the same place as the data from Hamilton *et al.*[21–23] and Shumway,[25] obtained in the 20- to 41-kHz range. This supports the argument for a simple relaxation-time model for the attenuation mechanism of sound in marine sediments.

The data of Fig. 2 show a bias toward higher values of relaxation time. This is probably due to the presence of some experimental errors, which normally tend to give higher values of attenuation. Extreme values in the data were eliminated by using Chauvenet's criterion. Any data points falling outside the range, such that the probability of occurrence is less than $1/2n$ (n being the number of points in a small interval), were discarded. Because of the culling process, 12 large values and 1 small value were discarded from the entire data set of 361 points. A curve given by

$$\tau = a(\phi - b)e^{-c(\phi - b)^d}, \qquad (15)$$

where ϕ is the mean grain diameter in phi units, and a, b, c, and d are constants to be evaluated, was fitted to the reduced data by a nonlinear least-squares method. This expression was chosen based on a careful observation of the trend in the data set. These constants were evaluated by an unconstrained nonlinear optimization method based on the Nelder–Meade simplex algorithm.[26] The constant d was 2.06, and so a convenient value of 2 was adopted. The rest of the constants were then recalculated. The curve fit yielded

$$\tau = 0.0848(\phi - 0.415)e^{-0.0437(\phi - 0.415)^2}\ \mu\text{s}. \qquad (16)$$

The data and the curve fit (Fig. 2) show an increase in relaxation time τ, with an increase in ϕ in the sand region

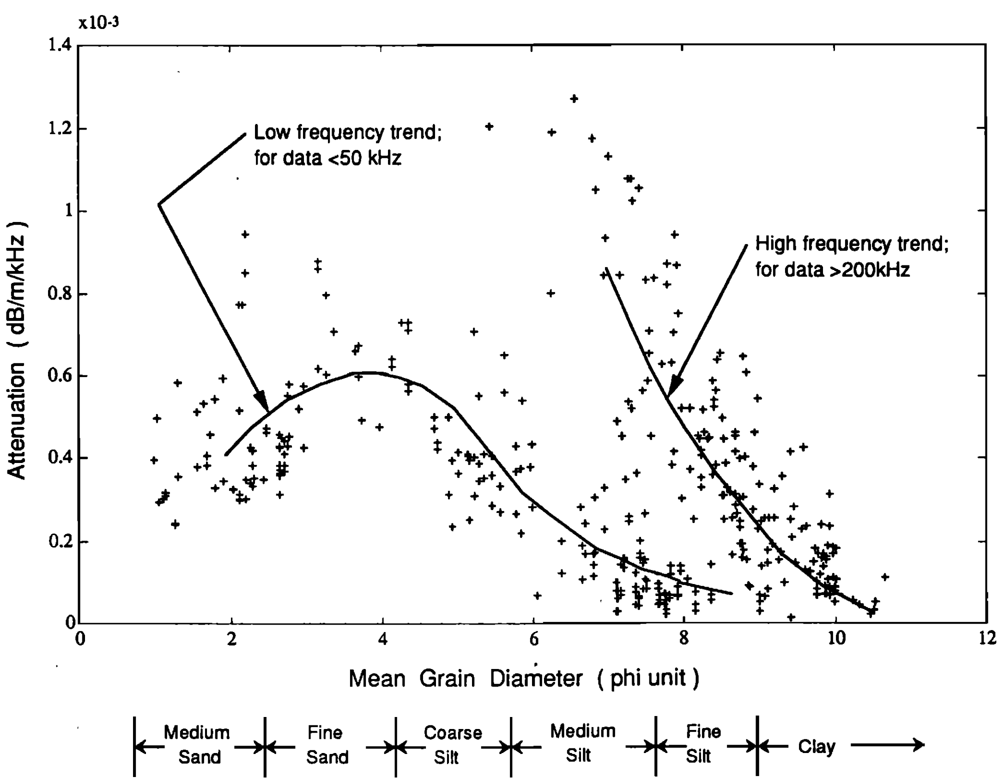

FIG. 1. Attenuation measurements (taken from Ref. 21–23, 25—low frequency, 20, 24—high frequency) for sediments with various mean grain sizes. Measurements were performed at different frequencies and adjusted to a linear frequency dependence (dB/m/kHz).

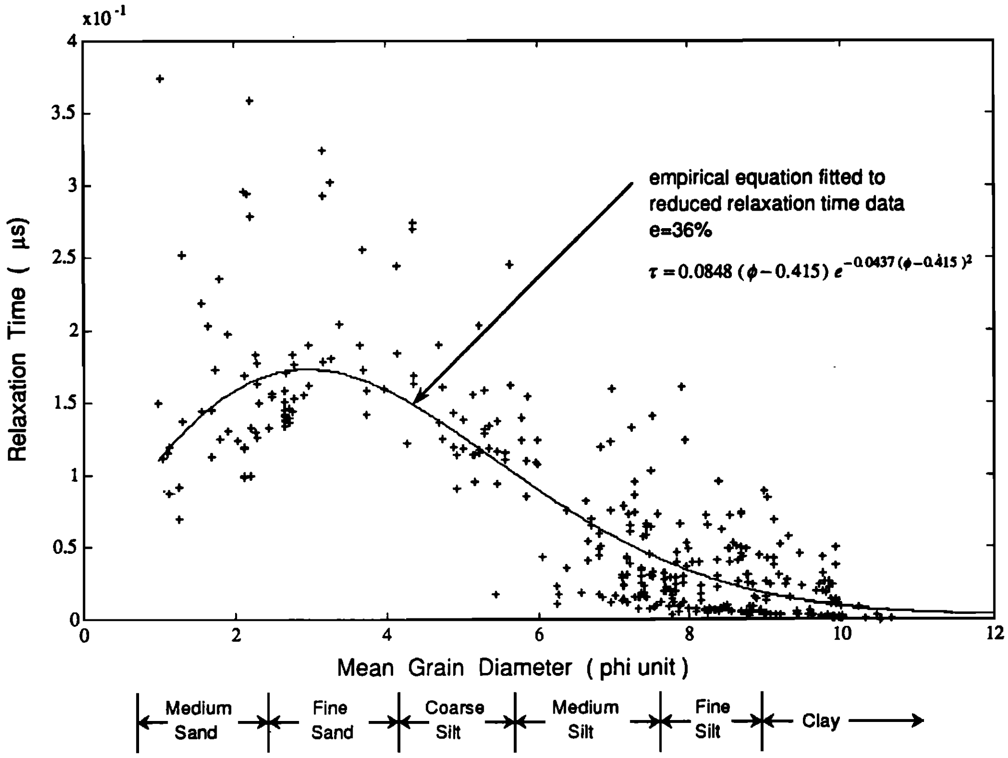

FIG. 2. Attenuation measurements (taken from Ref. 20–25), adjusted to equivalent relaxation time values and plotted as a function of mean grain size.

with the maximum observed at fine sand. A similar trend in the attenuation coefficient is reported by various investigators (Hamilton,[23] McCann and McCann,[24] and Shumway[25]). With further increase in ϕ, τ decreases sharply in the silt region and then drops gradually in the clay region. Table I, obtained by averaging the reduced data in the region of each sediment type, gives representative values of relaxation time for various types of marine sediments. Figure 3 shows the variation of attenuation with frequency for sand ($\tau = 0.16\ \mu s$), silt ($\tau = 0.06\ \mu s$), and clay ($\tau = 0.02\ \mu s$) obtained from Eq. (6). In measuring attenuation with the chirp sonar, a nominal velocity of 1500 m/s is used. As previously mentioned [see discussion under Eq. (10)], at low frequencies (< 100 kHz), relaxation time can be measured experimentally without requiring the knowledge of the speed of sound in the sediment sample.

III. ATTENUATION OF THE CHIRP SONAR PULSE

The relaxation-time model was used to study the dispersion and attenuation characteristics of the correlated chirp sonar pulse. Chirp sonar[17] is a frequency-modulated, computerized, quantitative sub-bottom profiler that produces high-resolution, low-noise, wideband acoustic signatures of the sub-bottom sediments. Using a measured impulse response of the entire transmitter and receiver components, the chirp sonar pulse observed at the output of the correlator is designed to have a Blackman–Harris spectral shape with a zero phase characteristic. Zero phase or linear phase (a time delay) results in the pulse being symmetrical about its peak value. But nonlinear phase, such as caused by phase dispersion acting on the pulse as it propagates through a lossy seabottom, modifies the pulse so that its time domain representation is no longer symmetrical. Figure 4 shows the effect of phase dispersion on the shape of a zero phase pulse after it has propagated through 40 m of sand, which was calculated by using only the imaginary part of the exponent in the expression for $H(\omega)$ [Eq. (12)]. The effect of phase dispersion on the symmetry of the zero phase pulse is hardly noticeable. The corresponding dispersed and attenuated pulse (Fig. 4) exhibits a pulse broadening. Compared to different types of pulses, the increase in the pulse width is least for a chirp pulse, which is attributed to the Blackman–Harris window shape of its spectrum. Figure 5 shows the increase in the pulse width for a correlated chirp pulse traveling through sandy, silty, and clayey sediments. Considering a 2- to 10-kHz chirp pulse, penetration achievable in a sandy bottom is around 20 m (40 m of two-way travel), the increase in the pulse width is less than 20% for most sediments. The resolution of the chirp pulse is not significantly reduced as the pulse propagates through the sediment. This is a major factor behind chirp sonar's ability to produce high-resolu-

TABLE I. Average relaxation time for different sediment types.

Sediment type	Relaxation time (μs)
Medium sand	0.15
Fine sand	0.17
Coarse silt	0.13
Medium silt	0.06
Fine silt	0.03
Clay	0.02

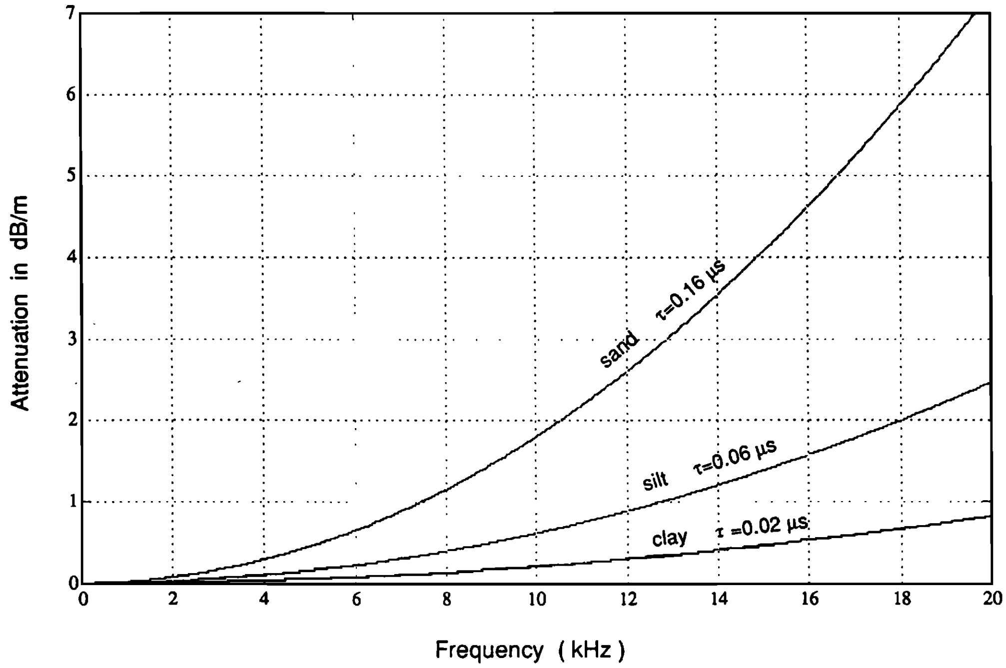

FIG. 3. Frequency dependence of attenuation of sound in various marine sediments for a relaxation-time model; based on a nominal sound velocity of 1500 m/s [see text under Eq. (10)].

tion images. Also, the above characteristics of the chirp sonar are useful for the accurate evaluation of the sediment impulse response by standard inversion algorithms, most of which neglect the distortion in the pulse shape due to the attenuation. Still, phase dispersion is observed for high-frequency pulses, as evident from Fig. 6, which shows a phase dispersed only, and a phase dispersed and attenuated pulse, after traveling through 10 cm of clay, for a 0.2- to 1.0-MHz frequency range.

IV. ATTENUATION ESTIMATION TECHNIQUE

The standard methods for the determination of attenuation in marine sediments are rise time,[10–12] spectral ratio,[10–14] spectrum modeling,[12] and wavelet modeling.[12,17] The rise-time method, although algebraically elegant, is of little practical use as it needs noise-free data. The spectral methods perform poorly when overlapping reflections constructively and destructively interfere at different frequencies

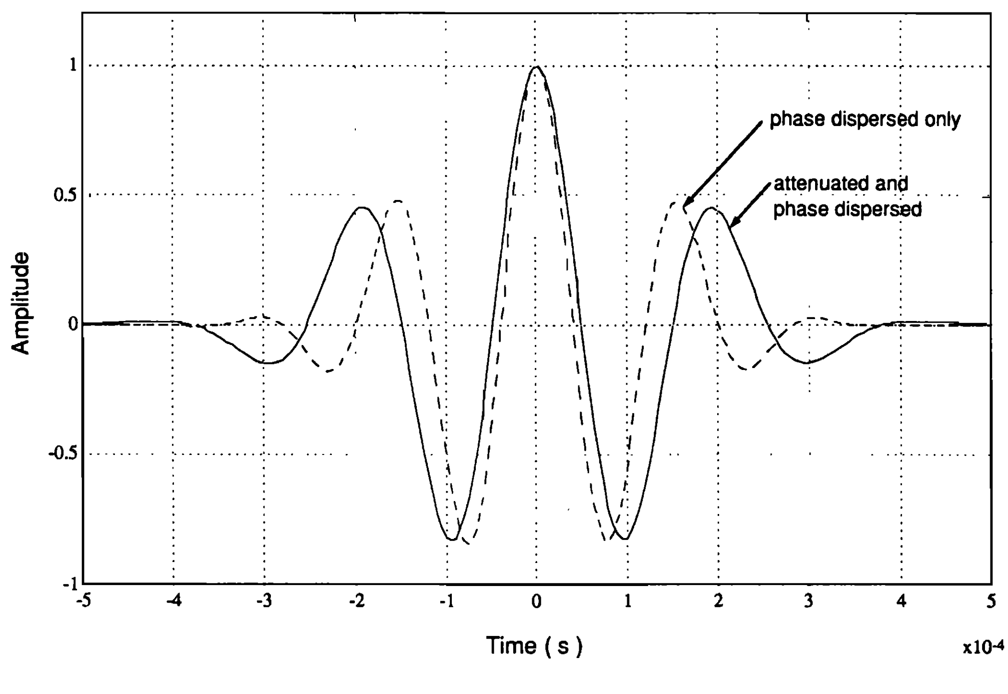

FIG. 4. Shape of a zero phase 2- to 10-kHz chirp pulse after propagating through 40 m of sand ($\tau = 0.16$ μs; pulse amplitudes are rescaled to 1).

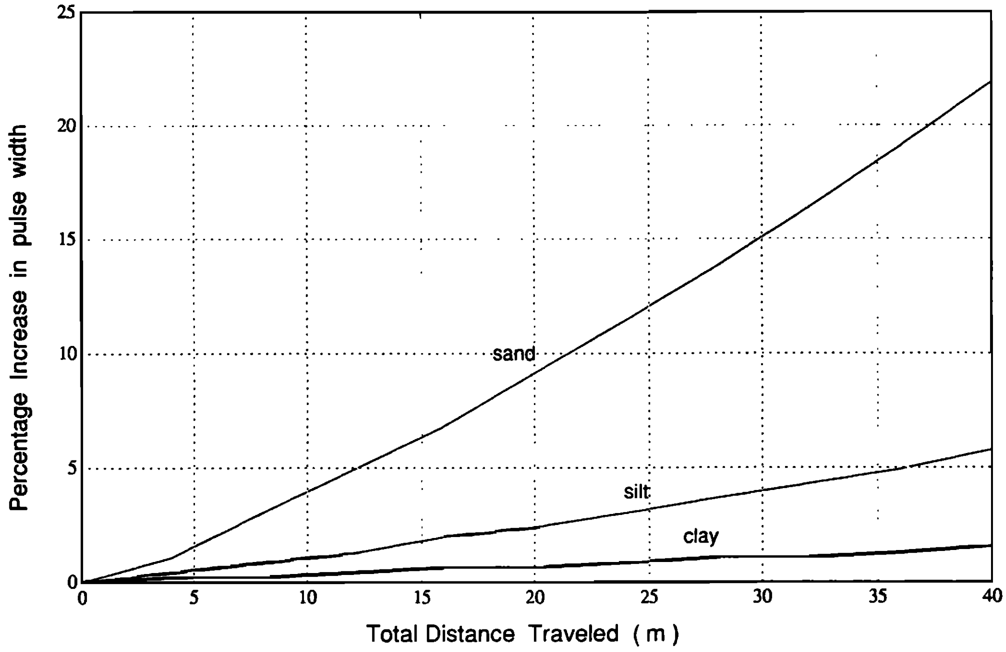

FIG. 5. Increase in pulse width for a 2- to 10-kHz pulse traveling through various marine sediments.

thereby introducing ripples in the spectrum. Also, the spectral methods are seriously affected by small changes in the location of the time gate. Only the wavelet modeling method[12,17] works to some extent for signals that do not overlap more than 60%. In this paper, we propose a new time domain method for estimating attenuation that overcomes these difficulties.

For a broadband source, the attenuated spectrum shifts to a lower frequency range because of the frequency selective transfer function of the attenuating medium. The method of measuring the shift in the center frequency of a broadband pulse has already been investigated by some researchers (Kuc[15] and Fink *et al.*[16]). These methods were used in estimating acoustic attenuation from reflected ultrasound signals. These investigators had considered three methods of estimation of the center frequency: (1) a correlation technique, (2) the mean of the spectral estimate, and (3) a zero crossing count analysis. When applied to the sonar data, the first two methods are adversely affected by overlapping reflections, whereas the zero crossing analysis is a crude meth-

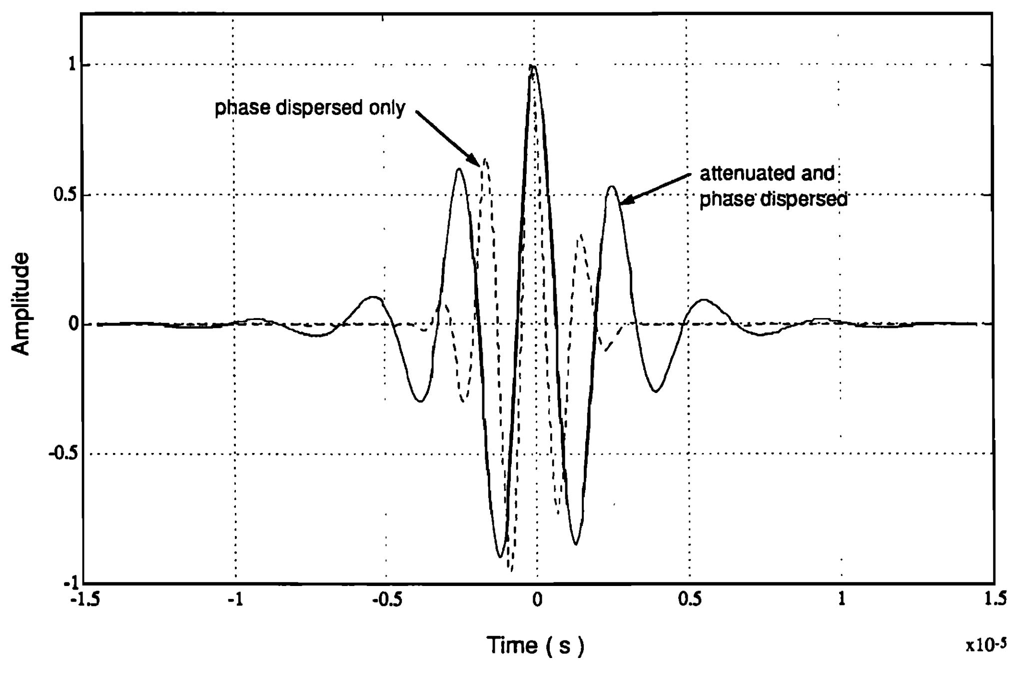

FIG. 6. Shape of a zero phase 0.2- to 1.0-mHz chirp pulse after propagating through 10 cm of clay ($\tau = 0.02$ μs; pulse amplitudes are rescaled to 1).

od and gives satisfactory result only for a long record length. Here, we propose that the center frequency can be estimated by using the instantaneous frequency of the analytic signal.

The complex analytic signal $z(t)$ is given by

$$z(t) = s(t) + j\hat{s}(t), \qquad (17)$$

where $s(t)$ is a real time signal (output of the correlator) and $\hat{s}(t)$ is the Hilbert transform of $s(t)$. The analytic signal $z(t)$ can be represented also by

$$z(t) = E(t)e^{j\phi(t)}, \qquad (18)$$

where $E(t)$ is the envelope function and $\phi(t)$ is the phase. Therefore, the phase $\phi(t)$ is given by

$$\phi(t) = -j\log[z(t)/E(t)]. \qquad (19)$$

In practice, phase unwrapping is required in the numerical evaluation of Eq. (19). Now, the instantaneous frequency is given by

$$f_i = \frac{1}{2\pi}\frac{\partial\phi}{\partial t}. \qquad (20)$$

The instantaneous frequency of the output of the chirp pulse correlator oscillates over the frequency range of the pulse spectrum. The oscillation of the instantaneous frequency of the received signal is stochastic because of the random phase and amplitude of the many reflected pulses arriving from volume scatterers within the marine sediment. Still, the local mean value of the instantaneous frequency will represent the center frequency of the spectrum and will steadily decrease as the pulse attenuates. The instantaneous frequency, being evaluated from the phase, which is a normalized quantity, is expected to be least influenced by the adverse effect of overlapping reflections.

The above technique was implemented numerically to develop tables for use in estimating the attenuation of marine sediments from the data collected by the chirp sonar. To relate the shift in the center frequency to attenuation, a numerical analysis of the attenuation characteristics of the correlated output pulse was carried out. The attenuated pulse amplitude spectrum, at the output of the correlator, is obtained by taking the absolute value of $Y(\omega)$ given in Eq. (13). The correlated pulse spectrum $S(\omega)$ is selected to have a 2- to 10-kHz Blackman–Harris spectral shape with zero phase, and the output pulse amplitude spectrum is given by

$$|Y(\omega)| = |S(\omega)|e^{-\alpha x}. \qquad (21)$$

Using Eq. (21) and the relaxation-time model given in Eq. (10), the chirp pulse was numerically attenuated. The median frequency of $|Y(\omega)|$ was calculated for various sediments. This method was used in our classification model as a simple means for measurement of the center frequency shift caused by the acoustic attenuation in the sediment. The median frequency is the value of frequency that divides the output pulse amplitude spectrum into two parts of equal areas: It is a measure of the location of the concentration of energy in the PSD. Figure 7 shows the expected shift in the center frequency for the chirp pulse traveling through sand, silt, and clay. The shift in the center frequency is significant and is a measurable quantity. For large values of relaxation time (e.g., for sand), the shift in center frequency exhibits a nonlinear behavior. Still, the penetration in sand being limited to about 20 m, a linear dependence between center frequency shift and travel distance can be assumed for convenience without introducing significant error. This assumption allowed us to relate frequency shift per meter to relaxation time of the sediment. This is presented in Fig. 8. The estimated relaxation time is then used to predict the sediment type by using Fig. 2.

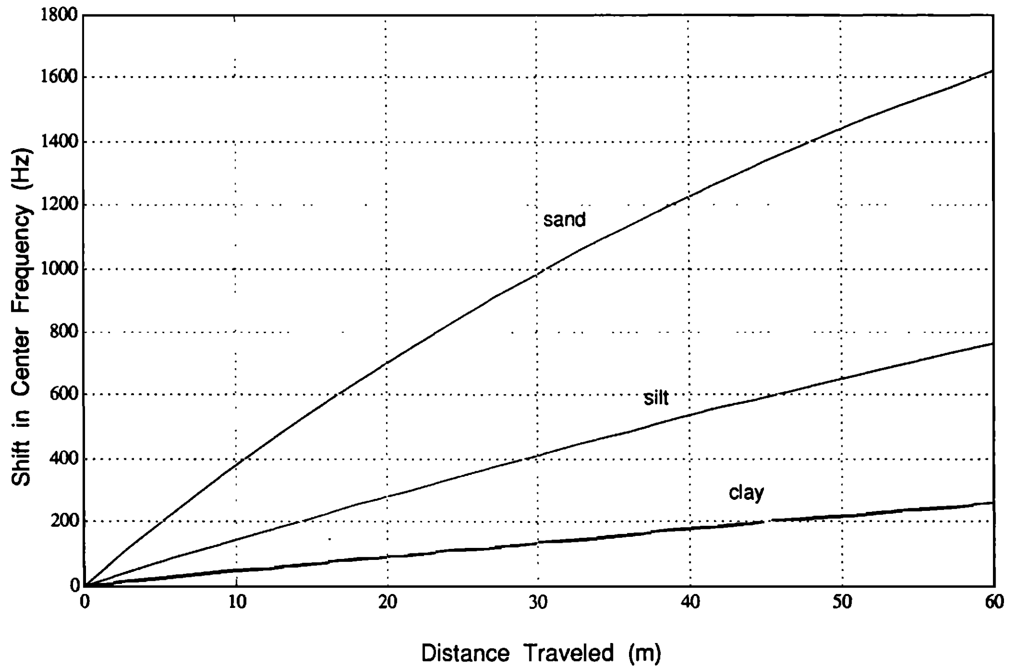

FIG. 7. Shift in center frequency of a 2- to 10-kHz chirp pulse propagating through various marine sediments; based on a nominal sound velocity of 1500 m/s [see text under Eq. (10)].

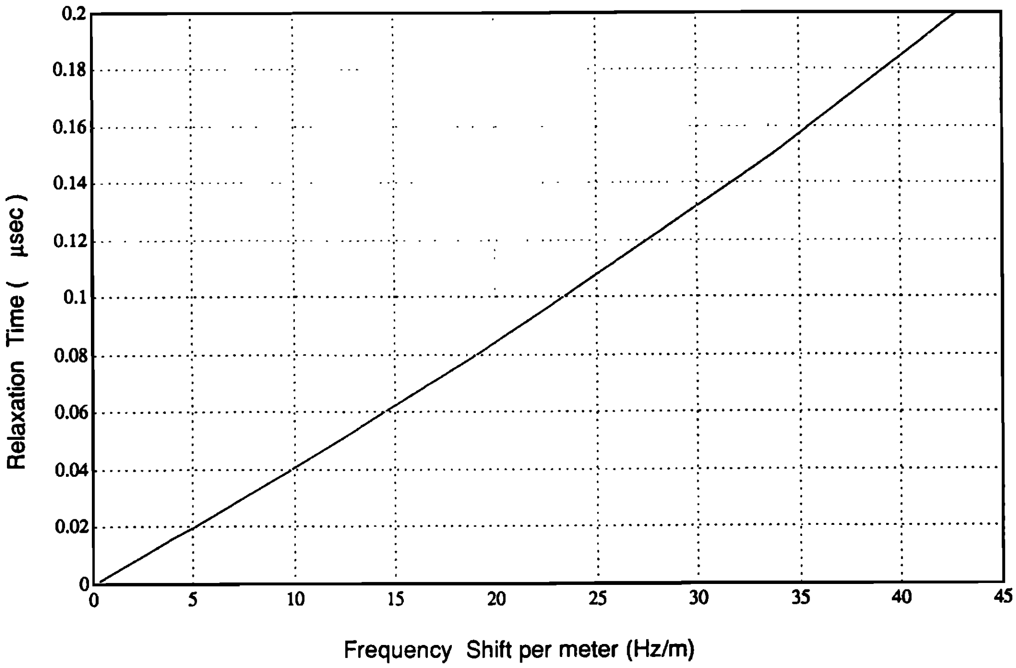

FIG. 8. Relaxation time as a function of shift in center frequency per meter of sediment (for a 2- to 10-kHz chirp pulse); based on a nominal sound velocity of 1500 m/s [see text under Eq. (10)].

V. FIELD RESULTS

A chirp sonar seafloor survey was carried out in the west passage of Narragansett Bay, RI in May 1990, and again in September 1990. The surficial sediments of Narragansett Bay have been studied by McMaster;[27] the distribution of sediment types in the West Passage is shown in Fig. 9. The chirp sonar system was set up and calibrated to transmit a 20-ms pulse ranging in frequency from 2–10 kHz at a rate of twice per second. In the first experiment, the system was calibrated by using large areas with known sediment type in Narragansett Bay. In the second experiment, a south–north line between Dutch Island and the Wickford breakwater wall and a west–east line between the Wickford breakwater and Hope Island were run with the chirp sonar (Fig. 9). Loran C navigation, with three calibration points along the ship's track, provided accuracy to within ± 10 m (in the absence of abrupt atmospheric changes). Grab sample cores were taken at nine selected sites in the same proximity of the May survey. Also, at seven of these sites, 100 returns of chirp sonar data were digitally recorded as the ship was drifting over the core sites. Later, the cores were analyzed for density and porosity.[28]

The sonar data obtained from the specific core sites were analyzed to estimate the relaxation time using the frequency shift method described above. The analytic signal (complex time series signal) is computed by the chirp sonar signal processor by discarding the negative half spectrum prior to taking the inverse Fourier transform. Later, phase ϕ and instantaneous frequency f_i are evaluated by using Eqs. (19) and (20), respectively. To reduce the amplitude of random oscillations of f_i that are caused by scattering from within the sediment, 20 returns were ensemble averaged. For core site number 9, the averaged instantaneous frequency is plotted in Fig. 10, where the time axis is converted to a depth axis based on a constant sound speed of 1500 m/s. The section corresponding to the negative depth represents the direct arrival and noise recorded prior to the bottom arrival, and, therefore, is of no interest. The instantaneous frequency shows a decreasing trend with increase in depth. A sudden increase in the instantaneous frequency corresponding to a depth of 12 m is identified as the arrival of the first multiple. Based on these observations, a line was least-squares fitted to a section of the data corresponding to 0- to 12-m depth. This provided us with an estimate of the center frequency of the sonar returns arriving from the scatterers within this section of sediment. At this site, the slope of the line (center frequency shift per meter) is 30.04 Hz/m with a standard error of $\pm 2\%$ at the 90% confidence level. Referring to Fig. 8, the corresponding relaxation time is $0.13\,\mu$s. In this case, there is an ambiguity in deciding the sediment type from the relaxation time versus grain size curve (Fig. 2). The sediment type could be either medium sand or coarse silt. The analysis of a 12-cm core at site 9 shows that the surficial layer is predominantly silt with an underlying layer of silty medium sand. The estimated relaxation time value from the sonar data suggest medium sand to a depth of 12 m at this site. This compares favorably with McMaster's[27] data. In this example, the reflectivity method is only useful for classifying the surface sediment, whereas the attenuation method provides information on the underlying material. The added information provided by the attenuation method could be helpful in many engineering applications such as dredging surveys, bridge placement, and resource assessment.

Table II lists the chirp sonar predicted sediment types and *in situ* sediment types obtained from the cores for all seven sites. The predicted sediment types, which have minor ambiguities at three sites, are mostly one step finer than the

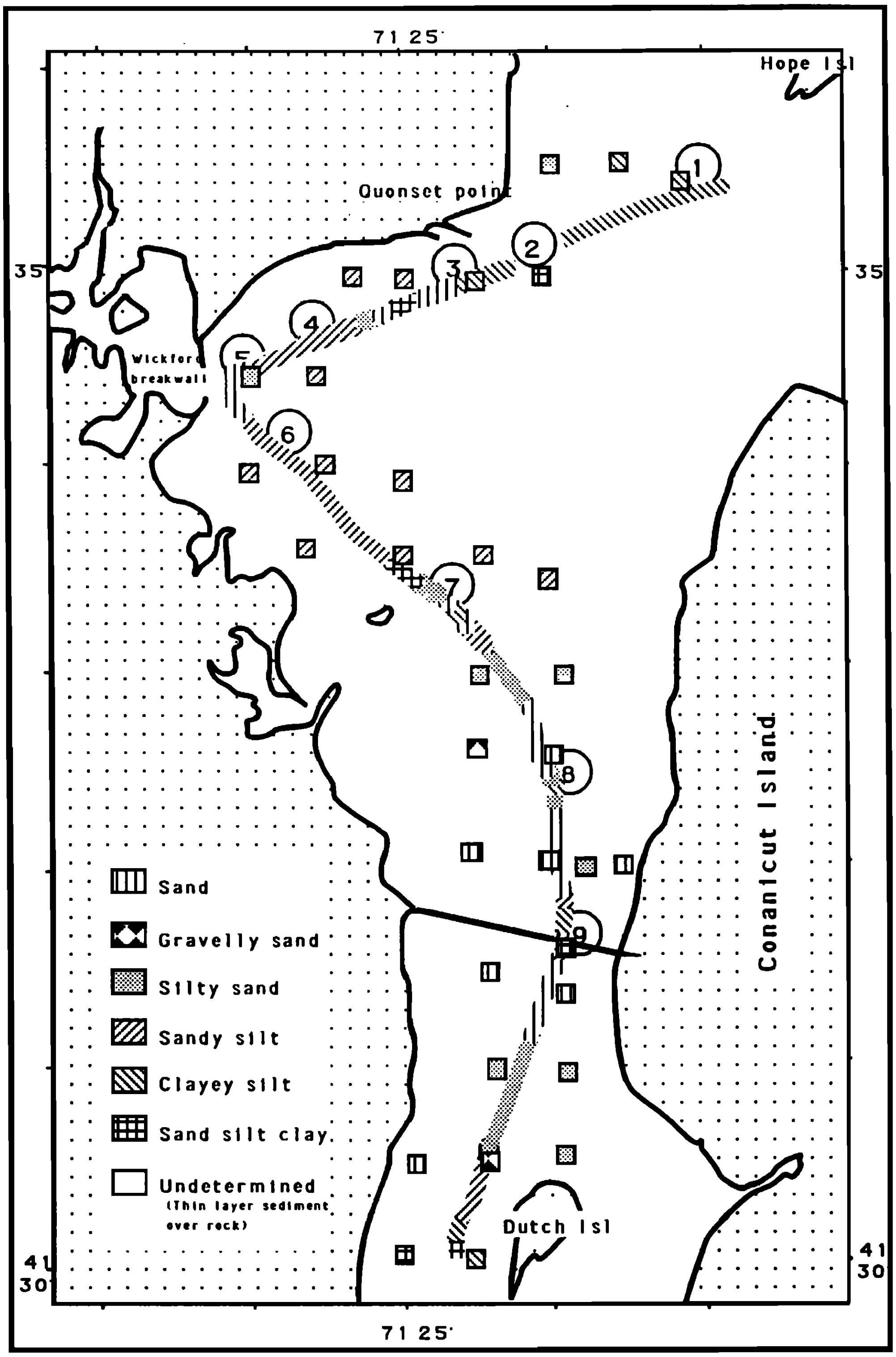

FIG. 9. Comparison of chirp sonar predicted sediment characteristics along the ship's track with core sites taken from McMaster (Ref. 27). Circles mark our core sites taken in Sept. 1990.

in situ sediment types. This implies that the predicted relaxation times are smaller than that obtained from the *in situ* sediment types using Fig. 2. Since the relation in Fig. 2 is based on measurements, it is believed that the small discrepancy could be due to experimental errors and/or disturbed core samples that biased the readings toward higher values.

VI. CONCLUSIONS

The suggested relaxation-time model for attenuation of sonar signals in marine sediments is supported by experimental data. The method is simplistic, in that it provides us with a single parameter characterizing attenuation in marine sediments. For low frequencies (<100 kHz), relaxation

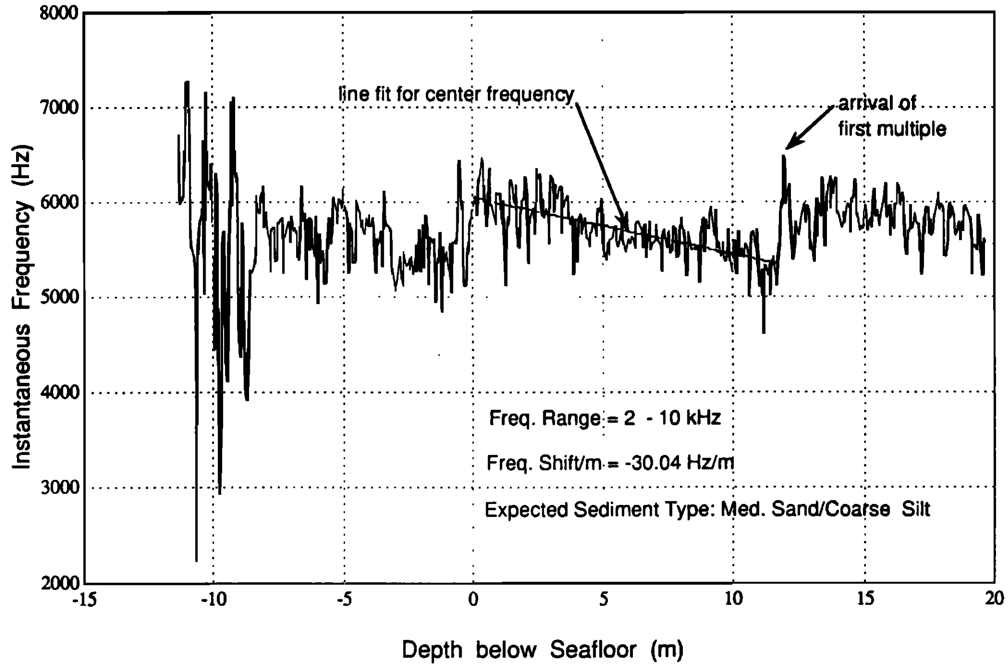

FIG. 10. Instantaneous frequency averaged over 20 sonar returns at site 9. Straight line regression provides shift in center frequency per meter of sediment; based on a nominal sound velocity of 1500 m/s [see text under Eq. (10)].

time can be estimated without requiring the knowledge of the sediment sound velocity. A new robust method using instantaneous frequency for estimating the attenuation of sonar pulses in sediment is used to classify submarine sediments to depths of up to 40 m. The repeatability of the chirp sonar pulse and *a priori* knowledge of its spectral content is used to implement a simple attenuation-based sediment classification procedure that operates in the time domain. Also, as the chirp sonar was originally designed to generate the analytic signal,[3] the use of the instantaneous frequency technique involves few additional computations and, therefore, can be implemented in real time. The sediment classification procedure can be improved by calibrating the method with the help of ground truth data over a wide range of marine sediment types.

TABLE II. Comparison of predicted sediment type with *in-situ* sediment type for various core sites.

Site No.	Estimated sediment type from cores	Predicted sediment type by chirp sonar
1	coarse silt	medium silt
4	coarse silt	medium silt
5	find sand	medium sand/ coarse silt
6	coarse silt	medium silt
7	medium sand	medium to coarse silt
8	medium to fine sand	medium sand/ coarse silt
9 (0–7 cm)	medium silt	medium sand/ coarse silt
9 (7–13 cm)	silty medium sand	

Independent reflectivity estimates of the sediment column will provide additional information to be used in a future model for improving sediment prediction reliability. Independent reflectivity estimates will also help to resolve any ambiguity in sediment type prediction that is based on relaxation time. Attenuation estimation, when used in concert with impedance estimation, is expected to provide us with a robust sediment classification scheme. Finally, this will provide better predictions of the geotechnical properties of marine sediments such as grain size distribution, porosity, density, and sound velocity.

ACKNOWLEDGMENT

This research was supported by the Office of Naval Research (Geo-Acoustics/Arctic Science Division; program manager, Dr. J. Kravitz) under Contract No. N00014-91-J-108.

[1] D. N. Lambert, "An evaluation of the Honeywell ELAC computerized sediment classification system," NORDA, Rep. No. 169 (1988).
[2] S. T. Knott, H. Hoskins, and E. O. LaCasce, Jr., "Estimation of the seabed acoustic impedance structure from normal-incident reflections: Somali Basin," J. Geophys. Res. **86**, 2935–2952 (1981).
[3] M. C. Rufino, "Microcomputer based chirp sonar; A real time shallow water seismic profiler," MS thesis, Ocean Engineering, University of Rhode Island, Kingston, RI (1990).
[4] M. A. Biot, "Theory of propagation of elastic waves in a fluid-saturated porous solid, I. Low-frequency range," J. Acoust. Soc. Am. **28**, 168–178 (1956).
[5] M. A. Biot, "Theory of propagation of elastic waves in a fluid-saturated porous solid, II. Higher frequency range," J. Acoust. Soc. Am. **28**, 179–191 (1956).
[6] M. A. Biot, "Mechanics of deformation and acoustic propagation in porous media," J. Appl. Phys. **33**(4), 1482–1498 (1962).
[7] M. A. Biot, "Generalized theory of acoustic propagation in porous dissipative media," J. Acoust. Soc. Am. **34**, 1254–1264 (1962).
[8] R. D. Stoll and G. M. Bryan, "Wave attenuation in saturated sediments," J. Acoust. Soc. Am. **47**, 1440–1447 (1970).
[9] R. D. Stoll, "Acoustic waves in ocean sediments," Geophysics **42**, 751–725 (1977).

[10] P. Tarif and T. Bourbie, "Experimental comparison between spectral ratio and rise time techniques for attenuation measurement," Geophys. Prospec. **35**, 668–680 (1987).
[11] M. Badri and H. M. Mooney, "*Q* measurements from compressional seismic waves in unconsolidated sediments," Geophysics **52**, 772–784 (1987).
[12] D. Jannsen, J. Voss, and F. Theilen, "Comparison of methods to determine *Q* in shallow marine sediments from vertical reflection seismograms," Geophys. Prospect. **33**, 479–497 (1985).
[13] P. S. Hauge, "Measurements of attenuation from vertical seismic profiles," Geophysics **46**, 1548–1558 (1981).
[14] R. S. Jacobson, G. G. Shor, Jr., and L. M. Dorman, "Linear inversion of body wave data-Part II: Attenuation versus depth using spectral ratios," Geophysics **46**, 152–162 (1981).
[15] R. Kuc, "Estimating acoustic attenuation from reflected ultrasound signals: Comparison of spectral-shift and spectral-difference approaches," IEEE Trans. ASSP **ASSP-32** (1), 1–6 (1984).
[16] M. Fink, F. Hottier, and J. F. Cardoso, "Ultrasonic signal processing for *in vivo* attenuation measurement: Short-time Fourier analysis," Ultrason. Imag. **5**, 117–135 (1983).
[17] S. G. Schock, L. R. LeBlanc, and L. A. Mayer, "Chirp sub-bottom profiler for quantitative sediment analysis," Geophysics **54**, 445–450 (1989).
[18] R. B. Lindsay, *Mechanical Radiation* (McGraw-Hill, New York, 1960).
[19] K. Aki and P. G. Richards, 1980, *Quantitative Seismology* (Freeman, San Francisco, 1980), Vol. I, pp. 172–177.
[20] S. Buchan, F. C. D. Dewes, A. S. G. Jones, D. M. McCann, and D. Taylor Smith, "The acoustic and geotechnical properties of North Atlantic Cores," University College of North Wales, Marine Science laboratories, (1971), Vols. 1 and 2.
[21] E. L. Hamilton, G. Shumway, H. W. Menard, and C. J. Shipek, "Acoustic and other physical properties of shallow-water sediments off San Diego," J. Acoust. Soc. Am. **28**, 1–15 (1956).
[22] E. L. Hamilton, H. P. Bucker, D. L. Keir, and J. A. Whitney, 1970, "Velocities of compressional and shear waves in marine sediments determined *in situ* from a research submersible," J. Geophys. Res. **75**, 4039–4049 (1970).
[23] E. L. Hamilton, "Compressional-wave attenuation in marine sediments," Geophysics **37**, 620–646 (1972).
[24] C. McCann and D. M. McCann, "The attenuation of compressional waves in marine sediments," Geophysics **34**, 882–892 (1969).
[25] G. Shumway, "Sound speed and absorption studies of marine sediments by a resonance method," Geophysics **25**, Part I—451–467, Part II—659–682 (1960).
[26] W. H. Press, B. P. Flannery, S. A. Teukolsky, and W. T. Vetterling, *Numerical Recipes* (Cambridge U.P., Cambridge, 1989).
[27] R. L. McMaster, "Sediments of Narragansett Bay system and Rhode Island Sound," J. Sediment. Petrol. **30**, 249–274 (1960).
[28] J. Peck, "Report on sediment property measurements of surficial samples from west passage, Narragansett Bay," Informal Report, GSO, University of Rhode Island, Kingston, RI (1991).